

# Chain-of-Focus: Adaptive Visual Search and Zooming for Multimodal Reasoning via RL

Xintong Zhang<sup>1,2\*</sup> Zhi Gao<sup>2,3\*</sup> Bofei Zhang<sup>2</sup> Pengxiang Li<sup>1,2</sup> Xiaowen Zhang<sup>2</sup> Yang Liu<sup>2</sup>  
Tao Yuan<sup>2</sup> Yuwei Wu<sup>1,4</sup> Yunde Jia<sup>4</sup> Song-Chun Zhu<sup>2,3,5</sup> Qing Li<sup>2</sup>

<sup>1</sup>Beijing Key Laboratory of Intelligent Information Technology,

School of Computer Science & Technology, Beijing Institute of Technology

<sup>2</sup>State Key Laboratory of General Artificial Intelligence, BIGAI

<sup>3</sup>School of Intelligence Science and Technology, Peking University

<sup>4</sup>Guangdong Laboratory of Machine Perception and Intelligent Computing, Shenzhen MSU-BIT University

<sup>5</sup>Department of Automation, Tsinghua University

cof-reasoning.github.io

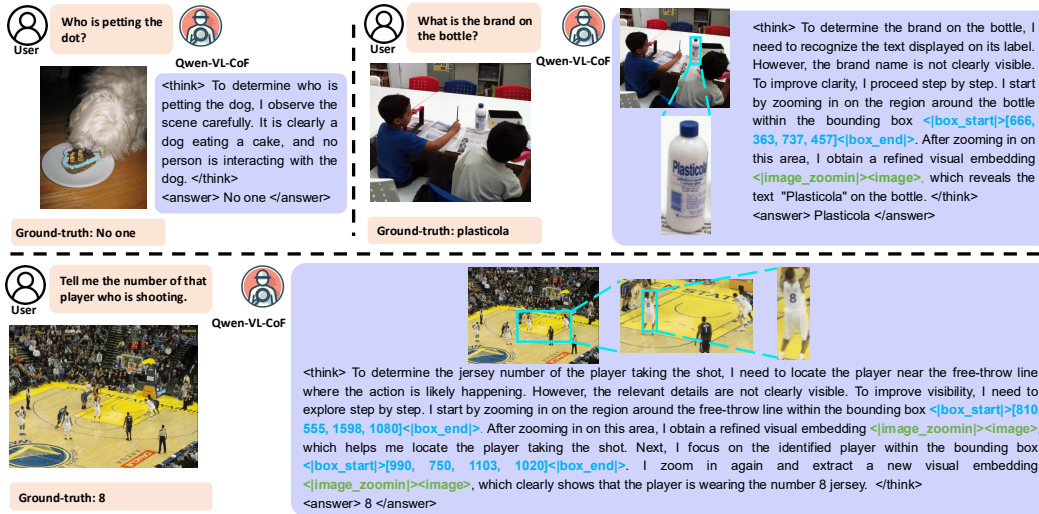


Figure 1: The proposed CoF method enables VLMs to perform adaptive search and reasoning to obtain a chain of key visual information for answering. Based on current visual tokens, the VLMs directly answer the question if the visual information is sufficient, otherwise, it zooms in on key regions for more details.

## Abstract

Vision language models (VLMs) have achieved impressive performance across a variety of computer vision tasks. However, the multimodal reasoning capability has not been fully explored in existing models. In this paper, we propose a Chain-of-Focus (CoF) method that allows VLMs to perform adaptive focusing and zooming in on key image regions based on obtained visual cues and the given questions, achieving efficient multimodal reasoning. To enable this CoF capability, we present a two-stage training pipeline, including supervised fine-tuning (SFT) and reinforcement learning (RL). In the SFT stage, we construct the MM-CoF dataset, comprising 3K samples derived from a visual agent designed to adaptively identify key regions to solve visual tasks with different image resolutions and questions. We use MM-CoF to fine-tune the Qwen2.5-VL model for cold start. In the RL stage, we leverage the outcome accuracies and formats as rewards to update the Qwen2.5-VL model, enabling further refining the model's search and reasoning

\*Equal contribution. ✉ Corresponding author.

strategy without human priors. Our model achieves significant improvements on multiple benchmarks. On the  $V^*$  benchmark that requires strong visual reasoning capability, our model outperforms existing VLMs by 5% among 8 image different resolutions ranging from  $\times 224$  to  $\times 4K$ , demonstrating the effectiveness of the proposed CoF method and facilitating the more efficient deployment of VLMs in practical applications.

## 1 Introduction

Vision language models (VLMs) that integrate visual encoders with large language models (LLMs) have made remarkable progress across various applications [30, 49, 43]. Notable open-source models such as LLaVA [23], InternVL [6], MiniCPM-V [42], and Qwen-VL [2] have achieved comparable performance with those of closed-source counterparts (*e.g.*, GPT-4o). These models typically extract visual tokens using visual encoders and combine them with textual tokens for predictions [25, 18, 1].

Developing multimodal reasoning capabilities is essential for building general-purpose vision-language models. However, most existing efforts primarily focus on enhancing reasoning within the natural language space. [12, 7, 47, 29, 19]. For example, VLMs may first analyze the objects, attributes, and background in images, then infer latent cues, and finally answer the question, where the whole process only uses natural language [13, 27, 40, 48, 44, 26]. Despite their impressive performance, relying solely on natural language for reasoning may pose limitations in visual perception, leading to the loss of critical information and suboptimal answering quality. For example, VLMs may attend to irrelevant regions or fail to capture fine-grained details in small areas of a fixed image, resulting in the omission of important visual cues and degraded reasoning performance.

In this paper, we propose the Chain-of-Focus (CoF) method that allows VLMs to perform adaptive search and zooming in on key image regions (see Fig. 1 for details), thus creating a chain of focus steps for multimodal reasoning with gradually obtained visual cues. For example, when the given image is high-resolution and uses a large number of visual tokens, or when the question depends on a large region of the image, the extracted visual tokens are often sufficient to answer the question directly. On the other hand, when the image is low-resolution with fewer visual tokens, or when the question demands details from small regions of the image, the visual tokens may not provide enough cues. In this case, the model should search for and zoom in on key image regions to extract more visual cues. In implementation, the visual tokens corresponding to key regions are appended to previously generated output tokens for subsequent outputs during a single generation round. This approach allows the VLMs to gather more visual cues, enabling them to analyze the image more thoroughly, accurately, and reliably than if they only relied on a static view of the image. Note that our method does not perform visual search and zooming for every image, but performs adaptive search and zooming based on obtained visual cues, reducing the cost while keeping the performance. Recently, OpenAI has released GPT-o3 and GPT-o4-mini that can think with images in their chain-of-thought, utilizing cropping and zooming techniques to integrate visual and textual reasoning [31]. This paper proposes a feasible way to reproduce the capability of GPT-o3 and GPT-o4-mini.

In the SFT stage, we introduce the MM-CoF dataset, constructed 3K data using the SAM [16] dataset and covering a variety of image resolutions. We first synthesize tasks for these randomly sampled images, and then build a visual agent equipped with multiple tools to perform visual search and reasoning on the images until the assigned task is completed. Subsequently, we prompt a large language model (LLM) to summarize the agent’s reasoning trajectory into a coherent CoF reasoning process for SFT. We fine-tune a Qwen2.5-VL-7B model using MM-CoF for cold start. In the RL stage, we leverage the outcome accuracies and formats as rewards to update the VLMs, enabling further refining the model’s search and reasoning strategy without human priors. We denote the obtained model as Qwen2.5-VL-7B-CoF. Experiments of Qwen2.5-VL-7B-CoF are conducted on multiple benchmarks, such as  $V^*$  [37], GQA, and DocVQA. Results show that the enhanced adaptive multimodal reasoning capabilities in our model lead to improved performance, surpassing original VLMs on a range of image resolutions from  $\times 224$  to  $\times 4K$ . These findings highlight the efficacy of the proposed CoF method, the MM-CoF dataset, and the two-stage training pipeline.

In summary, our contributions are three-fold. (1) We propose the Chain-of-Focus (CoF) method that significantly improves the visual reasoning ability of VLMs. (2) We introduce a data collection pipeline to efficiently collect CoF data via a visual search agent, leading to MM-CoF, a dataset containing 3K CoF samples across diverse domains, image resolutions, and questions. (3) We develop

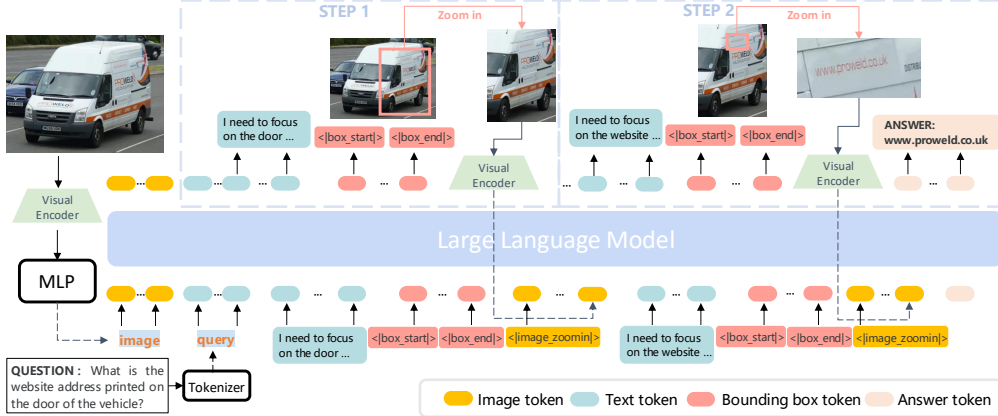


Figure 2: Illustration of the chain-of-focus framework. The textual tokens are in blue, visual tokens are in yellow, bounding box tokens are in red, and answer tokens are in orange. `<|box_start|>`, `<|box_end|>`, and `<|image_zoomin|>` are special tokens. Coordinates are represented in text.

a Qwen2.5-VL-7B-CoF model, an advanced VLM that could perform adaptive visual search and reasoning on images, leading to thorough, accurate, and reliable visual understanding.

## 2 Related Work

### 2.1 Vision Language Models

Developing powerful VLMs is a hot research topic in the multimodal learning community [25]. Existing VLMs combine a visual encoder (*e.g.*, ViT [9]), an LLM (*e.g.*, Qwen-2.5 [39]), and a projector (*e.g.*, MLP or Q-Former [18]) that connects the visual encoder and LLM for multimodal understanding. The visual encoder encodes images into visual tokens, and the projector converts the visual tokens into the language space. Finally, the visual tokens and textual tokens are combined and fed into the LLM for autoregressive prediction. Recent models, such as LLaVA-OneVision [17], InternVL [6], Qwen-VL [2], and LLaVA-UHD [38] have shown that using high-resolution images significantly improves the performance of visual perception and reasoning. Compared to low-resolution images, high-resolution images contain more details, and processing high-resolution images usually requires more visual tokens, delivering more visual cues [24, 15]. Different from existing methods that feed high-resolution images at first, our method performs adaptive search to identify and zoom in on key regions in a chain of focus, avoiding processing irrelevant regions for cost reduction and improving the reasoning capability of VLMs.

### 2.2 Multimodal Reasoning

Reasoning is an efficient scheme in LLMs, improving the interpretability and reliability in generation [36, 46, 11]. However, extending the reasoning ability to VLMs is still an open problem. Some methods write visual reasoning demonstrations that guide VLMs to understand complex tasks and capture relationships in images via in-context learning (ICL) [45, 29, 12, 10, 7]. To scale up the reasoning ability of VLMs, some methods update the model via supervised fine-tuning or reinforcement learning [27, 40, 48, 44, 26]. To further improve the reasoning ability, some methods collect reasoning data containing both the visual and textual information.  $V^*$  [37], CogCom [32], VPD [13], Visual CoT [33], DualFocus [3], and Chain-of-Spot [28] are representative methods that collect bounding boxes of key objects in images, then involve them in the reasoning trace, and finally use these traces to fine-tune VLMs. When inferring, the VLMs perform a multi-round generation process, where VLMs first output bounding boxes of key objects, then crop the objects, and the VLMs re-answer the question based on the cropped images. Compared with existing methods that exhaustively search the entire image for every question, the proposed CoF method adopts a two-stage training strategy using supervised fine-tuning (SFT) and reinforcement learning (RL) to enable adaptive visual search and reasoning based on the available visual cues and the granularity of the question. It dynamically decides whether the current visual input suffices to answer the question or if further reasoning and zooming in are needed. This selective approach reduces computational cost while maintaining strong performance. The combination of SFT and RL further improves generalization across diverse multimodal tasks.

### 3 Chain-of-Focus

#### 3.1 Formulation

CoF empowers VLMs with multimodal reasoning in a one-round generation process, where VLMs may locate the key regions and output responses in multiple steps. The  $i$ -th step is formulated as

$$\max \pi_{\theta}(r_i, y_i | I, x, h_i), \quad (1)$$

where  $\pi_{\theta}$  denotes a VLM,  $I$  denotes the input image,  $x$  is the question,  $r_i$  and  $y_i$  denote the searched key regions and generated responses in the  $i$ -th step,  $r_i$  is optimal,  $r_i = [[c_1, c_2, c_3, c_4], \dots]$  contains coordinates of bounding boxes of key regions and  $y_i$  is in the textual format (if these regions can directly answer the question  $x$ ,  $y_i$  is the predicted answer, otherwise  $y_i$  is the reasoning content).  $h_i$  is the history of previous steps, including key regions, responses, and visual tokens corresponding to key regions,  $h_i = [r_1, y_1, o_1, r_2, y_2, o_2, \dots]$ ,  $o_i$  denotes the appended visual tokens.

#### 3.2 Architecture

The overall process of CoF is shown in Fig. 2, which is constructed on top of VLMs. The VLMs adopt the same architecture as commonly used VLMs (e.g., Qwen-VL), including a vision encoder, a projector, and an LLM. The visual encoder extracts visual tokens, the projector projects these visual tokens to the same space as textual tokens, and the LLM generates outputs based on visual tokens and textual tokens.

The bounding box of  $[x_1, y_1, x_2, y_2]$  can be represented using its top-left coordinate  $(x_1, y_1)$  and bottom-right coordinate  $(x_2, y_2)$ . We represent a single bounding box by concatenating its four coordinates with two special tokens,  $\langle |box\_start| \rangle$  and  $\langle |box\_end| \rangle$ , resulting in the format:  $\langle |box\_start| \rangle [x_1, y_1, x_2, y_2] \langle |box\_end| \rangle$ . These two special tokens are pretrained in Qwen-2.5-VL. Note that in one step of CoF, multiple key regions may be identified, leading to multiple bounding boxes being predicted. However, not all bounding boxes require zooming in. Only regions that need further exploration are zoomed in.

To indicate which bounding boxes require zooming in, we introduce a special token  $\langle |image\_zoomin| \rangle$ , which signals that the visual content within the corresponding region should be zoomed in and that region-specific visual tokens should be inserted. This special token is added to the tokenizer during stage 1 of the LoRA-based supervised fine-tuning. After identifying the bounding boxes that require zoom-in, we incorporate the corresponding visual information into the model’s input by performing the following steps: (1) crop the key regions indicated by each bounding box; (2) resize them to the model’s input resolution; (3) encode them using the visual encoder to obtain visual tokens, denoted as  $o_j$  for the  $j$ -th bounding box; and (4) concatenate these tokens with the special token  $\langle |image\_zoomin| \rangle$  and append them to the previously generated output tokens. CoF supports interleaved reasoning over both visual and textual inputs. As illustrated in Fig. 2, the input representation at the later step includes both types of tokens, based on which the VLM generates the next sequence of outputs.

Please first think through the reasoning process before answering the question. If the relevant area of the image is unclear or difficult to see, first locate the region by generating a bounding box in the following format:  $\langle |box\_start| \rangle [x1, y1, x2, y2] \langle |box\_end| \rangle$ . Then, use the  $\langle |image\_zoomin| \rangle$  tag to zoom in on that region for closer inspection. Present your reasoning process and answer enclosed within these tags:  $\langle think \rangle$  reasoning process here  $\langle /think \rangle$   $\langle answer \rangle$  answer here  $\langle /answer \rangle$ .  $\langle image \rangle$  Question: What is the website address printed on the door of the vehicle

$\langle think \rangle$  To determine the website address printed on the door of the vehicle, I need to focus on the website text, but it is not clearly visible. To improve visibility, I proceed step by step. I first locate the door of the vehicle and obtain the bounding box  $\langle |box\_start| \rangle [x_1, y_1, x_2, y_2] \langle |box\_end| \rangle$ . After zooming in on this region, I obtain a refined visual embedding  $\langle |image\_zoomin| \rangle o_0$ . However, the website is still unclear. I further narrow the bounding box to focus specifically on the text area, yielding  $\langle |box\_start| \rangle [x_1, y_1, x_2, y_2] \langle |box\_end| \rangle$ , and obtain a new visual embedding  $\langle |image\_zoomin| \rangle o_1$ . Now I can clearly read the text: www.proweld.co.uk.  $\langle /think \rangle$   $\langle answer \rangle$  www.proweld.co.uk  $\langle /answer \rangle$

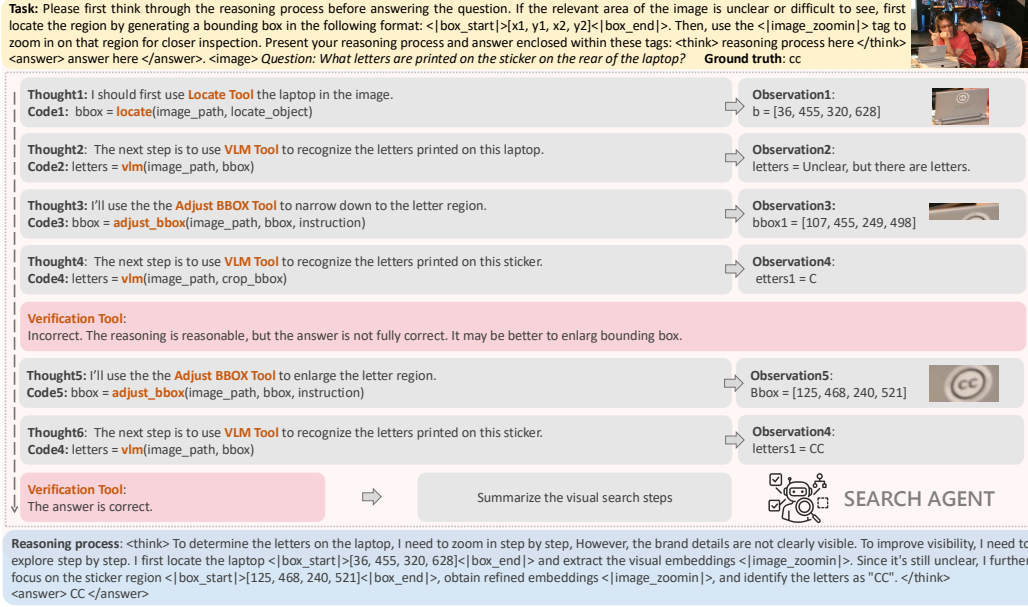


Figure 3: The proposed data collection pipeline. We develop a visual search agent that progressively locates regions necessary for answering the question. Sampled questions, images, and answers from the source datasets combined with the prompt are denoted in yellow. The reasoning steps of the agent are shown in pink. The summarized chain-of-focus reasoning process is shown in blue.

### 3.3 Training

We utilize a two-stage training pipeline, including supervised fine-tuning (SFT) and reinforcement learning (RL). We apply the collected CoF data to train the Qwen2.5-VL-7B model, which uses the ViT model as the visual encoder, a two-layer multilayer perceptron as the projector, and Qwen2.5-7B as the LLM. The input resolutions to Qwen2.5-VL-7B are sampled from a list  $\{224, 336, 448, 672, 1024, 1920, 2560, 3840\}$ .

In the SFT stage, we freeze the ViT parameters and apply LoRA fine-tuning to the remaining components, including the multilayer perceptron and the LLM. Concretely, we are given a training dataset  $\mathbb{D}$ , and a  $n$ -step CoF data is represented as  $(I, x, Y = \{r_1, y_1, o_1, \dots, r_n, y_n\})$ , where  $Y$  is a completed reasoning process of  $n$  steps to solve the question  $x$ . We fine-tune the Qwen2.5-VL-7B model, and the training objective is the cross-entropy loss.

$$\min_{\theta} \mathbb{E}_{(I, x, Y) \sim \mathbb{D}} \left[ - \sum_{i=2}^n \log \pi_{\theta}(r_i, y_i | I, x, \{r_j, y_j, o_j\}_{j=1}^{i-1}) \right], \quad (2)$$

where the visual embeddings  $o_i$  for key regions  $r_i$  are generated during training.

In the RL stage, we utilize the GRPO algorithm [34] for policy optimization. For each input question  $x$  and image  $I$ , GRPO samples a group of  $G$  reasoning processes  $\{Y_1, Y_2, \dots, Y_G\}$ . The trained policy  $\pi_{\theta}$  is then updated by maximizing the following objective,

$$\mathcal{J}_{\text{GRPO}}(\theta) = \mathbb{E}_{(I, x, h_i) \sim \mathbb{D}, \{Y_i\}_{i=1}^G \sim \tau_{\text{old}}(\cdot | q; \mathcal{E})} \left[ \frac{1}{G} \sum_{i=1}^G \frac{1}{\sum_{t=1}^{|Y_i|} \mathbb{I}(Y_{i,t})} \sum_{t=1}^{|Y_i|} \mathbb{I}(Y_{i,t}) \cdot \min \left( p_t \hat{A}_{i,t}, \text{clip} \left( p_t, 1 - \epsilon, 1 + \epsilon \right) \hat{A}_{i,t} \right) \right] - \beta \mathbb{D}_{\text{KL}}[\pi_{\theta} \| \pi_{\text{ref}}], \quad (3)$$

where  $p_t = \frac{\pi_{\theta}(Y_{i,t} | I, x, Y_{i, <t-1>}; \mathcal{R})}{\pi_{\text{old}}(Y_{i,t} | I, x, Y_{i, <t-1>}; \mathcal{R})}$ ,  $Y_{i,t}$  denotes the  $t$ -th token in  $Y_i$ ,  $\hat{A}_{i,t}$  denotes the advantage at  $Y_{i,t}$ , computed based on the relative ranking of rewards within the group,  $\beta$  controlling the KL-regularization strength. The clipping threshold  $\epsilon$  ensures stable updates.

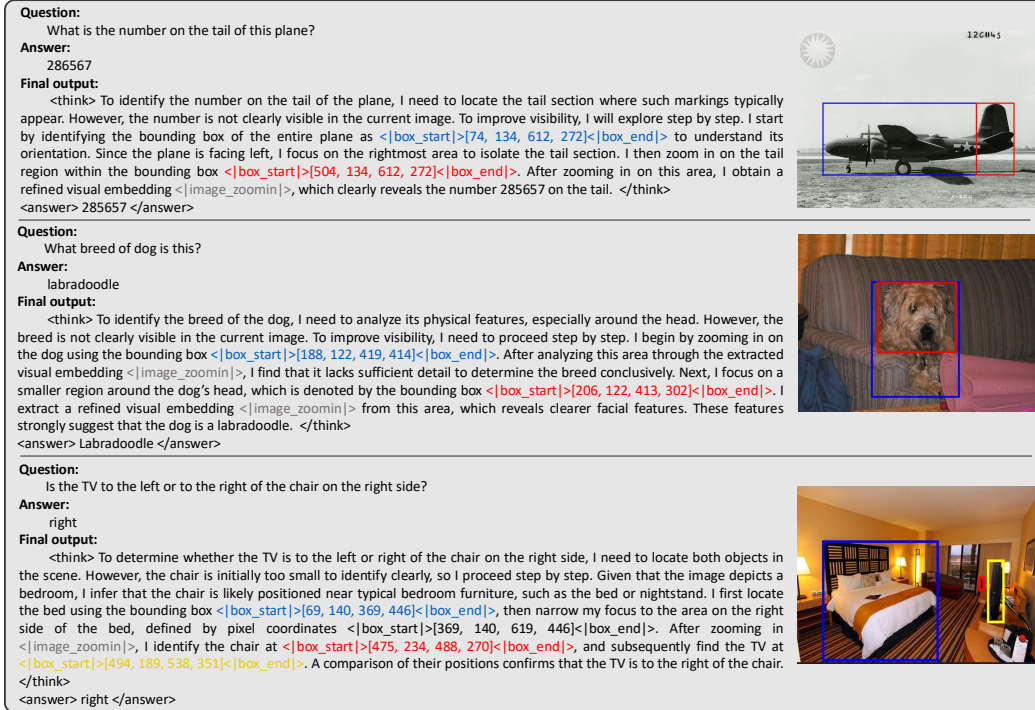


Figure 4: Examples of our generated CoF data via the visual search agent. Bounding boxes in red, blue, and yellow denote image regions focused in the first, second, and third steps, respectively.

Reward signals serve as the optimization objective and directly guide the behavior of the policy model during training. Here we use rule-based rewards, combined with the answer correctness and format correctness,

$$r = r_{correct} + r_{format}, \quad (4)$$

where  $r_{correct} = 1$  if the answer is correct, otherwise  $r_{correct} = 0$ . Similarly,  $r_{format} = 1$  if the response is in the `<think></think><answer></answer>` format, otherwise  $r_{format} = 0$ .

We mask out the visual tokens  $o_j$  between `<image_zoomin>` and `</image_zoomin>` from the loss computation. This prevents external tokens from the loss calculations, ensuring training stability and preserving the model’s inherent reasoning sequences from disruption.

## 4 Dataset

This section presents the MM-CoF dataset, outlining its data collection pipeline and analysis. We randomly select images from the SA\_1B dataset[16], which are usually high-resolution.

### 4.1 Question-Answering Generation

We randomly select 360 images from the SA\_1B dataset and upscale them to a resolution of 4K to present sufficient visual details. Using GPT-4.1, we generate four questions per image. To ensure answer accuracy, we use both GPT-4.1 and Qwen-2.5-VL-72B to answer each question, and retain only those QA pairs where both models produce consistent answers, resulting in approximately 1,000 high-quality QA pairs.

To explore different reasoning patterns, each image is resized to multiple resolutions (ranging from  $\times 224$  to  $\times 4K$ ), and Qwen-2.5-VL-72B is prompted to assess whether the question can be directly answered at each resolution, along with providing an answer. This process is repeated five times per resolution, and only QA pairs with consistent judgments are retained. If the model consistently judges the question to be directly answerable and provides the correct answer, the pair was categorized as not requiring zoom-in; otherwise, it is considered to require zoom-in reasoning. In total, we obtain 2,201 QA pairs that require zoom-in reasoning and 2,294 that can be answered directly. These samples reflect two main reasoning patterns: (1) The same question across different image resolutions exhibits varying zoom-in requirements. A question requires zoom-in for correct answering at low

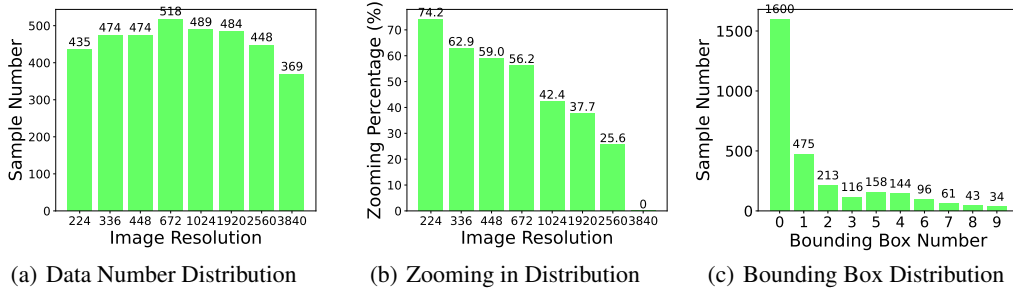


Figure 5: Data statistics of MM-CoF.

resolutions but becomes directly answerable at higher resolutions, or remains consistently either answerable or unanswerable regardless of resolution (i.e., questions that either require zooming in or do not); (2) Different questions about the same image exhibit varying zoom-in requirements. For QA pairs that require zoom-in reasoning, we further use an automated agent to obtain the corresponding step-by-step reasoning process. For those that can be answered directly without zooming in, we prompt GPT-4.1 to construct the reasoning process accordingly.

## 4.2 Visual Search Agent

We build a visual search agent using the React framework [41], which uses GPT-4.1-mini as a controller and performs step-by-step reasoning, as shown in Fig. 3. In each step, the controller outputs thoughts and Python code, calls tools by executing the code, and obtains the results of this step as observations. Our agent integrates three tools: the object detection tool, the bounding box adjusting tool, the multimodal understanding tool, and the verification tool.

Concretely, we extract a sample from the source dataset and send a prompt containing the question and the ground-truth answer to the agent. Note that only the verification tool has access to the ground-truth answer, all other tools involved in the exploration process operate solely based on the visual content and the question. The agent performs step-by-step reasoning: it gradually locates key regions, refines the selected areas to precisely capture the relevant visual details necessary for answering the question, and invokes the multimodal understanding tool to generate an answer based on these regions. The verification tool evaluates both the predicted answer and the reasoning trajectory. If the predicted answer aligns with the ground truth, the reasoning process is summarized ref into a logically coherent and complete explanation using DeepSeek-V3[22]. Otherwise, the verification tool analyzes the previous reasoning steps and provides feedback and suggestions to guide further exploration. The agent then continues the reasoning process until it either finds the correct answer or reaches the maximum number of allowed reasoning steps.

The proposed data generation pipeline employs an agent equipped with multiple tools to infer or estimate key regions for accurately answering questions, rather than directly detecting objects. Based on the responses and feedback from the multimodal understanding tool, the agent dynamically adjusts the size and boundaries of the bounding boxes. This pipeline enables the use of contextual information and historical reasoning traces, while a verification step helps capture question-relevant signals and provides suggestions for refining the reasoning regions. Additionally, our dataset includes explicit reasoning steps for iteratively grounding and adjusting regions, thereby enhancing the step-by-step reasoning capabilities of VLMs. In scenarios where objects are particularly small or lack clear visual boundaries (e.g., textual regions without salient objects), the pipeline leverages the agent’s tool-using and reasoning capabilities to achieve more accurate region grounding.

Several representative examples collected via our pipeline are shown in Fig. 4. In the first example, the agent identifies the plane’s tail using object detection and inference. In the second, since the dog’s breed is hard to determine directly, the agent reasons about regions likely to contain breed-specific features and locates the dog’s head through trial and error. In the third, as the chair is too small for direct detection, the agent infers the region where the chair is likely to appear and uses spatial reasoning to locate both the chair and the nearby TV.

These cases highlight the challenge of identifying key regions that cannot be detected by standard object detectors, showcasing our agent’s ability to ground informative regions through tool use, spatial reasoning, and common sense.

Table 1: Accuracy comparisons on  $V^*$  with baselines using different image resolutions (*Img Res.*).

Method / <i>Img Res.</i>	224	336	448	672	1024	1920	2560	3840
Qwen2.5-VL-7B	40.4	41.4	49.7	60.7	71.7	76.2	80.3	84.1
Qwen2.5-VL-SFT	41.2	43.2	49.6	62.1	71.4	76.7	84.3	85.2
Qwen2.5-VL-7B-CoF	<b>42.9</b>	<b>48.7</b>	<b>52.9</b>	<b>70.7</b>	<b>73.9</b>	<b>80.4</b>	<b>88.2</b>	<b>89.3</b>

Table 2: Accuracy comparisons on benchmarks with baselines.

Method	TextVQA	m3cot	$V^*$	POPE
BLIP2 [18]	42.5	-	37.7	85.3
Instruct-BLIP [8]	50.7	-	34.0	78.9
Qwen-VL [2]	63.8	-	45.8	84.7
MiniGPT-v2 [4]	-	-	33.2	80.5
Qwen2.5-VL-7B	<b>83.6</b>	64.4	80.0	86.2
Qwen2.5-VL-7B-CoF	81.8	<b>66.6</b>	<b>88.0</b>	<b>88.4</b>

### 4.3 Dataset Analysis

In this case, we collect three pieces of data in total. We provide three key statistics: word number, bounding box number, and bounding box scale. **Data Number.** The data numbers of different image resolutions is shown in Fig. 5(a). We can find that different image resolutions have similar data numbers, showing that the dataset is balanced among image resolutions, avoiding overfitting to a specific resolution. **Zooming Distribution.** The zooming distribution of each image resolution is shown in Fig. 5(a). As the resolution increases, the amount of data that needs zooming in for accurate answering decreases, which is consistent with common sense. **Bounding Box Number.** We measure the number of bounding boxes in the response, as shown in Fig. 5(c). Most cases have zero bounding box, since there are half of the data that does not require zooming. As the number of bounding boxes increases, the amount of data decreases, showing that most cases require a non-long reasoning path.

## 5 Experiments

### 5.1 Setting

We utilize multiple datasets, including TextVQA [35], m3cot [5],  $V^*$  [37], and POPE [20]. We apply CoF to the Qwen2.5-VL-7B model, obtain the Qwen2.5-VL-7B-CoF model, and compare its performance with the original Qwen2.5-VL-7B model. In addition, we also compare our model with several visual reasoning methods that use the same input resolution as ours.

**Training Details.** We train 1 epoch for SFT. The learning rate is  $2e - 5$  for the LLM backbone and projector,  $2e - 6$  for ViT. The batch size is 8 per device. After the SFT stage, we denote the model as Qwen2.5-VL-7B-SFT. We train 2000 steps for RL. The learning rate is  $1e-6$  for the LLM backbone and projector,  $1e-6$  for ViT. The batch size is 1 per device. We sample 5 rollouts in solving each task. After the RL stage, we denote the model as Qwen2.5-VL-7B-CoF.

### 5.2 Accuracy

We first evaluate the performance of Qwen2.5-VL-7B-CoF on  $V^*$  using different image resolutions, and the experimental results are shown in Tab. 1. We can observe that, compared with the original Qwen2.5-VL-7B model, Qwen2.5-VL-7B-SFT has better performance across different image resolutions. The reason is that our MM-CoF dataset contains grounding and chain-of-focus information, leading to better visual perception, search, and reasoning abilities for VLMs. Comparing

Table 3: Accuracy comparisons on benchmarks with multimodal reasoning methods.

Method	TextVQA	m3cot	$V^*$	POPE
VisCoT [33]	77.5	-	-	86.5
VOCOT [21]	-	-	58.4	86.6
SEAL [37]	-	-	75.4	82.4
CoS [14]	65.0	-	-	86.4
PaLI-3-VPD [13]	63.7	-	-	87.7
Qwen2.5-VL-7B-CoF	<b>81.8</b>	<b>66.6</b>	<b>88.0</b>	<b>88.4</b>



Figure 6: Case studies of Qwen2.5-VL-7B-CoF on three examples.

Qwen2.5-VL-7B-SFT with the Qwen2.5-VL-7B-CoF model, Qwen2.5-VL-7B-CoF further improves the performance, showing its effectiveness.

We then compare our Qwen2.5-VL-7B-CoF model with the original Qwen2.5-VL-7B model and the SFT model Qwen2.5-VL-7B-SFT on multiple benchmarks, as shown in Tab. 2. Our models have consistent improvements on multiple benchmarks, showing that the two-stage training pipeline can further improve the generalization of models, leading to a general multimodal reasoning ability.

We further compare our Qwen2.5-VL-7B-CoF model with existing multimodal reasoning methods, including VisCoT [33], VOCOT [21], SEAL [37], CoS [14], and PaLI-3-VPD [13]. Results are shown in Tab. 3. Our method achieves comparable performance among these visual chain-of-thought methods. Regarding efficiency, they do not consider the inference cost issue, while our CoF method has the reasoning ability and reduces inference costs.

### 5.3 Grounding

We evaluate the grounding ability of our VLMs. We randomly select 100 testing data from  $V^*$ , and evaluate the grounding ability in the reasoning process by human check. The results are shown in Tab. 4. Similar to the accuracy performance, the RL training stage brings 4 % improvements, showing the effectiveness of the used two-stage training pipeline.

### 5.4 Visualization

In Fig. 6, we visualize 6 examples to illustrate the CoF process in the Qwen2.5-VL-7B-CoF model. We observe that Qwen2.5-VL-7B-CoF can well locate key regions for details, especially for small objects and non-object regions. It can also gradually locate key regions via reasoning. Based on these regions, the model then correctly answers the given questions.

Table 4: Grounding evaluation in the multimodal reasoning process.

Method	Accuracy
Qwen2.5-VL-7B-SFT	0.82
Qwen2.5-VL-7B-CoF	<b>0.86</b>

## 6 Conclusion

In this paper, we have presented the chain-of-focus (CoF) method to improve the multimodal reasoning ability of VLMs via adaptive search and focus. By operations of adaptive image zooming, the CoF method can help the reasoning process using more visual cues. The proposed data collection pipeline can efficiently collect CoF data and the data can indeed empower the perception, grounding,

and reasoning ability for visual language models. The used SFT-RL training pipeline can gradually improve the generalization of VLMs.

**Limitations.** In this work, we only collect question-answering data for CoF, which may limit the other capabilities of models, such as captioning and visual dialogue. In the future, we will develop a more cheap and automated data collection pipeline, through which the proposed CoF method could be efficiently adapted to diverse domains.

## References

- [1] Jean-Baptiste Alayrac, Jeff Donahue, Pauline Luc, Antoine Miech, Iain Barr, Yana Hasson, Karel Lenc, Arthur Mensch, Katherine Millican, Malcolm Reynolds, et al. Flamingo: a visual language model for few-shot learning. *NeurIPS*, 35:23716–23736, 2022.
- [2] Jinze Bai, Shuai Bai, Shusheng Yang, Shijie Wang, Sinan Tan, Peng Wang, Junyang Lin, Chang Zhou, and Jingren Zhou. Qwen-vl: A frontier large vision-language model with versatile abilities. *arXiv preprint arXiv:2308.12966*, 2023.
- [3] Yuhang Cao, Pan Zhang, Xiaoyi Dong, Dahua Lin, and Jiaqi Wang. Dualfocus: Integrating macro and micro perspectives in multi-modal large language models. *arXiv preprint arXiv:2402.14767*, 2024.
- [4] Jun Chen, Deyao Zhu, Xiaoqian Shen, Xiang Li, Zechun Liu, Pengchuan Zhang, Raghuraman Krishnamoorthi, Vikas Chandra, Yunyang Xiong, and Mohamed Elhoseiny. Minigt-v2: large language model as a unified interface for vision-language multi-task learning. *arXiv preprint arXiv:2310.09478*, 2023.
- [5] Qiguang Chen, Libo Qin, Jin Zhang, Zhi Chen, Xiao Xu, and Wanxiang Che. M3cot: A novel benchmark for multi-domain multi-step multi-modal chain-of-thought. *arXiv preprint arXiv:2405.16473*, 2024.
- [6] Zhe Chen, Jiannan Wu, Wenhai Wang, Weijie Su, Guo Chen, Sen Xing, Muyan Zhong, Qinglong Zhang, Xizhou Zhu, Lewei Lu, et al. Internvl: Scaling up vision foundation models and aligning for generic visual-linguistic tasks. In *CVPR*, pages 24185–24198, 2024.
- [7] Zhenfang Chen, Qinhong Zhou, Yikang Shen, Yining Hong, Zhiqing Sun, Dan Gutfreund, and Chuang Gan. Visual chain-of-thought prompting for knowledge-based visual reasoning. In *Proceedings of the AAAI Conference on Artificial Intelligence*, volume 38, pages 1254–1262, 2024.
- [8] Wenliang Dai, Junnan Li, Dongxu Li, Anthony Tiong, Junqi Zhao, Weisheng Wang, Boyang Li, Pascale Fung, and Steven Hoi. InstructBLIP: Towards general-purpose vision-language models with instruction tuning. In *NeurIPS*, 2023.
- [9] Alexey Dosovitskiy, Lucas Beyer, Alexander Kolesnikov, Dirk Weissenborn, Xiaohua Zhai, Thomas Unterthiner, Mostafa Dehghani, Matthias Minderer, G Heigold, S Gelly, et al. An image is worth 16x16 words: Transformers for image recognition at scale. In *International Conference on Learning Representations*, 2020.
- [10] Zhi Gao, Yuntao Du, Xintong Zhang, Xiaojuan Ma, Wenjuan Han, Song-Chun Zhu, and Qing Li. Clova: A closed-loop visual assistant with tool usage and update. In *CVPR*, pages 13258–13268, 2024.
- [11] Zhi Gao, Bofei Zhang, Pengxiang Li, Xiaojuan Ma, Tao Yuan, Yue Fan, Yuwei Wu, Yunde Jia, Song-Chun Zhu, and Qing Li. Multi-modal agent tuning: Building a vlm-driven agent for efficient tool usage. In *ICLR*.
- [12] Tanmay Gupta and Aniruddha Kembhavi. Visual programming: Compositional visual reasoning without training. In *CVPR*, pages 14953–14962, 2023.
- [13] Yushi Hu, Otilia Stretcu, Chun-Ta Lu, Krishnamurthy Viswanathan, Kenji Hata, Enming Luo, Ranjay Krishna, and Ariel Fuxman. Visual program distillation: Distilling tools and programmatic reasoning into vision-language models. In *CVPR*, pages 9590–9601, 2024.
- [14] Ziyuan Huang, Kaixiang Ji, Biao Gong, Zhiwu Qing, Qinglong Zhang, Kecheng Zheng, Jian Wang, Jingdong Chen, and Ming Yang. Accelerating pre-training of multimodal llms via chain-of-sight. *arXiv preprint arXiv:2407.15819*, 2024.
- [15] Drew A Hudson and Christopher D Manning. Gqa: A new dataset for real-world visual reasoning and compositional question answering. In *CVPR*, pages 6700–6709, 2019.
- [16] Alexander Kirillov, Eric Mintun, Nikhila Ravi, Hanzi Mao, Chloe Rolland, Laura Gustafson, Tete Xiao, Spencer Whitehead, Alexander C Berg, Wan-Yen Lo, et al. Segment anything. In *ICCV*, pages 4015–4026, 2023.
- [17] Bo Li, Yuanhan Zhang, Dong Guo, Renrui Zhang, Feng Li, Hao Zhang, Kaichen Zhang, Yanwei Li, Ziwei Liu, and Chunyuan Li. Llava-onevision: Easy visual task transfer. *arXiv preprint arXiv:2408.03326*, 2024.
- [18] Junnan Li, Dongxu Li, Silvio Savarese, and Steven Hoi. Blip-2: Bootstrapping language-image pre-training with frozen image encoders and large language models. In *International Conference on Machine Learning (ICML)*, pages 19730–19742, 2023.

- [19] Pengxiang Li, Zhi Gao, Bofei Zhang, Tao Yuan, Yuwei Wu, Mehrtash Harandi, Yunde Jia, Song-Chun Zhu, and Qing Li. Fire: A dataset for feedback integration and refinement evaluation of multimodal models. In *The Thirty-eight Conference on Neural Information Processing Systems Datasets and Benchmarks Track*.
- [20] Yifan Li, Yifan Du, Kun Zhou, Jinpeng Wang, Wayne Xin Zhao, and Ji-Rong Wen. Evaluating object hallucination in large vision-language models. *arXiv preprint arXiv:2305.10355*, 2023.
- [21] Zejun Li, Ruipu Luo, Jiwen Zhang, Minghui Qiu, and Zhongyu Wei. Vocot: Unleashing visually grounded multi-step reasoning in large multi-modal models. *arXiv preprint arXiv:2405.16919*, 2024.
- [22] Aixin Liu, Bei Feng, Bing Xue, Bingxuan Wang, Bochao Wu, Chengda Lu, Chenggang Zhao, Chengqi Deng, Chenyu Zhang, Chong Ruan, et al. Deepseek-v3 technical report. *arXiv preprint arXiv:2412.19437*, 2024.
- [23] Haotian Liu, Chunyuan Li, Yuheng Li, and Yong Jae Lee. Improved baselines with visual instruction tuning. In *CVPR*, pages 26296–26306, 2024.
- [24] Haotian Liu, Chunyuan Li, Yuheng Li, Bo Li, Yuanhan Zhang, Sheng Shen, and Yong Jae Lee. Llava-next: Improved reasoning, ocr, and world knowledge, January 2024.
- [25] Haotian Liu, Chunyuan Li, Qingyang Wu, and Yong Jae Lee. Visual instruction tuning. In *NeurIPS*, volume 36, 2024.
- [26] Zhiyuan Liu, Yuting Zhang, Feng Liu, Changwang Zhang, Ying Sun, and Jun Wang. Othink-mr1: Stimulating multimodal generalized reasoning capabilities via dynamic reinforcement learning. *arXiv preprint arXiv:2503.16081*, 2025.
- [27] Ziyu Liu, Zeyi Sun, Yuhang Zang, Xiaoyi Dong, Yuhang Cao, Haodong Duan, Dahua Lin, and Jiaqi Wang. Visual-rft: Visual reinforcement fine-tuning. *arXiv preprint arXiv:2503.01785*, 2025.
- [28] Zuyan Liu, Yuhao Dong, Yongming Rao, Jie Zhou, and Jiwen Lu. Chain-of-spot: Interactive reasoning improves large vision-language models. *arXiv preprint arXiv:2403.12966*, 2024.
- [29] Chancharik Mitra, Brandon Huang, Trevor Darrell, and Roei Herzig. Compositional chain-of-thought prompting for large multimodal models. In *CVPR*, pages 14420–14431, 2024.
- [30] OpenAI. Gpt-4v(ision) system card. 2023.
- [31] OpenAI. Openai o3 and o4-mini system card. 2025.
- [32] Ji Qi, Ming Ding, Weihang Wang, Yushi Bai, Qingsong Lv, Wenyi Hong, Bin Xu, Lei Hou, Juanzi Li, Yuxiao Dong, et al. Cogcom: Train large vision-language models diving into details through chain of manipulations. *arXiv preprint arXiv:2402.04236*, 2024.
- [33] Hao Shao, Shengju Qian, Han Xiao, Guanglu Song, Zhuofan Zong, Letian Wang, Yu Liu, and Hongsheng Li. Visual cot: Advancing multi-modal language models with a comprehensive dataset and benchmark for chain-of-thought reasoning. *arXiv preprint arXiv:2403.16999*, 2024.
- [34] Zhihong Shao, Peiyi Wang, Qihao Zhu, Runxin Xu, Junxiao Song, Xiao Bi, Haowei Zhang, Mingchuan Zhang, YK Li, Y Wu, et al. Deepseekmath: Pushing the limits of mathematical reasoning in open language models. *arXiv preprint arXiv:2402.03300*, 2024.
- [35] Amanpreet Singh, Vivek Natarajan, Meet Shah, Yu Jiang, Xinlei Chen, Dhruv Batra, Devi Parikh, and Marcus Rohrbach. Towards vqa models that can read. In *CVPR*, pages 8317–8326, 2019.
- [36] Jason Wei, Xuezhi Wang, Dale Schuurmans, Maarten Bosma, Fei Xia, Ed Chi, Quoc V Le, Denny Zhou, et al. Chain-of-thought prompting elicits reasoning in large language models. volume 35, pages 24824–24837, 2022.
- [37] Penghao Wu and Saining Xie.  $v^*$ : Guided visual search as a core mechanism in multimodal llms. In *CVPR*, pages 13084–13094, 2024.
- [38] Ruyi Xu, Yuan Yao, Zonghao Guo, Junbo Cui, Zanlin Ni, Chunjiang Ge, Tat-Seng Chua, Zhiyuan Liu, Maosong Sun, and Gao Huang. Llava-uhd: an lmm perceiving any aspect ratio and high-resolution images. *arXiv preprint arXiv:2403.11703*, 2024.
- [39] An Yang, Baosong Yang, Beichen Zhang, Binyuan Hui, Bo Zheng, Bowen Yu, Chengyuan Li, Dayiheng Liu, Fei Huang, Haoran Wei, et al. Qwen2.5 technical report. *arXiv preprint arXiv:2412.15115*, 2024.
- [40] Yi Yang, Xiaoxuan He, Hongkun Pan, Xiyan Jiang, Yan Deng, Xingtao Yang, Haoyu Lu, Dacheng Yin, Fengyun Rao, Minfeng Zhu, et al. R1-onevision: Advancing generalized multimodal reasoning through cross-modal formalization. *arXiv preprint arXiv:2503.10615*, 2025.
- [41] Shunyu Yao, Jeffrey Zhao, Dian Yu, Nan Du, Izhak Shafran, Karthik Narasimhan, and Yuan Cao. React: Synergizing reasoning and acting in language models. In *ICLR*, 2023.
- [42] Yuan Yao, Tianyu Yu, Ao Zhang, Chongyi Wang, Junbo Cui, Hongji Zhu, Tianchi Cai, Haoyu Li, Weilin Zhao, Zhihui He, et al. Minicpm-v: A gpt-4v level mllm on your phone. *arXiv preprint arXiv:2408.01800*, 2024.

- [43] Shukang Yin, Chaoyou Fu, Sirui Zhao, Ke Li, Xing Sun, Tong Xu, and Enhong Chen. A survey on multimodal large language models. *arXiv preprint arXiv:2306.13549*, 2023.
- [44] Jingyi Zhang, Jiaying Huang, Huanjin Yao, Shunyu Liu, Xikun Zhang, Shijian Lu, and Dacheng Tao. R1-vl: Learning to reason with multimodal large language models via step-wise group relative policy optimization. *arXiv preprint arXiv:2503.12937*, 2025.
- [45] Yuechen Zhang, Shengju Qian, Bohao Peng, Shu Liu, and Jiaya Jia. Prompt highlighter: Interactive control for multi-modal llms. In *CVPR*, pages 13215–13224, 2024.
- [46] Zhuosheng Zhang, Aston Zhang, Mu Li, and Alex Smola. Automatic chain of thought prompting in large language models. *arXiv preprint arXiv:2210.03493*, 2022.
- [47] Ge Zheng, Bin Yang, Jiabin Tang, Hong-Yu Zhou, and Sibeï Yang. Ddcot: Duty-distinct chain-of-thought prompting for multimodal reasoning in language models. *Advances in Neural Information Processing Systems*, 36:5168–5191, 2023.
- [48] Hengguang Zhou, Xirui Li, Ruochen Wang, Minhao Cheng, Tianyi Zhou, and Cho-Jui Hsieh. R1-zero's "aha moment" in visual reasoning on a 2b non-sft model. *arXiv preprint arXiv:2503.05132*, 2025.
- [49] Deyao Zhu, Jun Chen, Xiaoqian Shen, Xiang Li, and Mohamed Elhoseiny. Minigpt-4: Enhancing vision-language understanding with advanced large language models. *arXiv preprint arXiv:2304.10592*, 2023.

## A Details of data generation

Our visual search agent is designed to perform visual search tasks guided by a well-structured prompt and in-context examples. The task prompt includes the task definition, a question, and the ground truth answer. The agent attempts to iteratively find the correct visual search path until its search results match the groundtruth or reach the maximum number of searches. At each step, it generates a thought and code based on the question and context, executes the code to obtain observations, and refines its reasoning path accordingly. A complete workflow is illustrated in the Fig. 7. To achieve this, we define specific modules that assist in the visual search process.

We design four modular tools based on Qwen-VL-Max, each driven by specialized prompts to support different stages of visual reasoning: Locate Tool, VLM Understanding Tool, Adjust BBox Tool, and Verification Tool.

- **Locate Tool:** Given an image, a target object description, and optionally a region of interest, the tool returns the bounding box of the specified object. This supports coarse-to-fine localization in cluttered or ambiguous scenes.
- **VLM Understanding Tool:** This module takes an image and a question as input, and uses the vision-language model to perform semantic understanding and generate a natural language answer with reasoning.
- **Adjust BBox Tool:** Given a current bounding box, a coordinate-guided reference image, and a textual instruction (e.g., "expand leftward", "shrink top edge"), the tool refines the bounding box accordingly.
- **Verification Tool:** This tool verifies whether the current output (answer or region) satisfies the question requirement. It also helps determine whether further zooming or refinement is necessary.

To control the workflow and integrate these modules effectively, we use GPT-4.1-mini as the controller. Unlike standard language models that rely solely on text-based descriptions of visual content, GPT-4.1-mini has the ability to directly perceive and analyze images. This allows it to understand image details more effectively and devise more reasonable plans for completing the task. Compared to other LLMs, GPT-4.1-mini demonstrates better decision-making and planning capabilities, especially when coordinating the use of vision modules.

To ensure the agent comprehends the functionality of each module and their integration, we present carefully crafted in-context examples. The system prompts and examples are respectively illustrated in Fig. 8, Fig. 9, Fig. 10, and Fig. 11. These examples demonstrate how the individual modules collaborate to accomplish the task.

## B Training details

The training parameters of our method are detailed in Tab. 5. The model is trained using 4 NVIDIA A100 GPUs, with a training time of 38 hours.

Configuration	Supervised finetuning	Reinforce learning
Tuning	Multilayer perception, LLM	Multilayer perception, LLM
Lora rank	32	-
Optimizer	AdamW	AdamW
Learning rate	1e-5	1e-6
Training Epochs	3	2
Global batch size	16	4
GPU Usage	4 NVIDIA A100	4 NVIDIA A100
Training Time	6h	32h

Table 5: Training details of two stages.

The accuracy score and reward during RL training are shown in Fig. 12, Fig. 13, and Fig. 14 as they vary with training steps.

User:



**Task:** Given an image, a question, continuously generate visual search steps and invoke tools based on the image content to answer the question.  
**Image\_path:** /home/2aa17ac35673beeb.jpg  
**Question:** What are the numbers on the closest plane?  
**Groundtruth:** 624

Search Agent:

Step 1

**Thought:** To determine the numbers on the closest plane, we need to follow these steps:  
 Locate the closest plane in the image.  
 Segment the area around the numbers on the closest plane.  
 Use OCR to identify the numbers on the closest plane. Let's start by locating the closest plane in the image using the locate tool.

**Agent is executing the code below:**  
`bboxes_closest_plane = locate(image_path="/home/2aa17ac35673beeb.jpg", crop_bbox=[], locate_object="plane")  
 print(bboxes_closest_plane)`

**Observation:** [[231, 174, 1023, 482], [127, 261, 366, 432], [14, 268, 233, 377], [126, 228, 660, 433]]



Step 2

**Thought:** Let's directly calculate the area within the code snippet without using a separate function. We'll create a list of areas and identify the bounding box with the largest area.

**Agent is executing the code below:**  
`bboxes_closest_plane = [[231, 174, 1023, 482], [127, 261, 366, 432], [14, 268, 233, 377], [126, 228, 660, 433]]  
 areas = [(bbox[2] - bbox[0]) * (bbox[3] - bbox[1])  
 for bbox in bboxes_closest_plane]  
 index_of_largest_area = areas.index(max(areas))  
 closest_plane_bbox = bboxes_closest_plane[index_of_largest_area]  
 print(closest_plane_bbox)`

**Observation:** [231, 174, 1023, 482]



Step 3

**Thought:** Now that we have determined the bounding box of the closest plane, the next step is to segment the area around the numbers on the closest plane. The numbers should be located on the body of the plane. We will use the VLM tool to recognize the numbers within this bounding box.

**Agent is executing the code below:**  
`closest_plane_bbox = [231, 174, 1023, 482]  
 numbers = vlm(image_path="/home/2aa17ac35673beeb.jpg", crop_bbox=closest_plane_bbox)  
 print(numbers)`

**Observation:** 624

**Verification tool:**  
 Correct, and the answer is correct and the reasoning process is reasonable.

**Summarize the reasoning process**  
**Final answer:**  
*<think> To identify the numbers on the closest plane, I first analyze the entire image to locate the closest plane. The bounding box for the closest plane is <box\_start> [231, 174, 1023, 482] <box\_end>. After zooming in, I get the refined visual embedding <image\_zoomin>, the correct answer to the question, "What are the numbers on the closest plane?" is 624. </think> <answer> 624 </answer>*

Figure 7: An example of visual search agent workflow.

You are an AI assistant. Given the bounding box (new\_bbox) (the red bounding box in the image), please use the guide lines and numeric markers to adjust the bounding box and complete the operation {operation}, helping to find the correct area to answer the question {question}.

If the operation is 'enlarge', make sure the adjusted bounding box fully contains the given bounding box.  
 Output the bounding box directly without extra words, for example: [x\_min, y\_min, x\_max, y\_max]

Figure 8: The prompt of the adjust bounding box tool.

You are an AI expert. You are given the question, the ground truth, the student's predicted answer, their visual search process, and the image.

Your task is to give a judgement evaluating a student's visual search process and predicted answer to a question, you need to evaluate the following aspects:

- Evaluate Answer Accuracy:
  - Evaluate whether the student's predicted answer is consistent with the ground truth. Ignore the minor differences in the predicted answer.
  - Consider the student's predicted answer is **\*\*correct\*\***, only if it is consistent with the **\*\*ground truth\*\***. Otherwise, consider it is **\*\*incorrect\*\***.
  - Only judge if the final answer is consistent with the ground truth; clearly output "Correct" or "Incorrect" without considering the reasoning process.
- Evaluate the visual Search process:
  - Judge whether the reasoning steps in the visual search process are logical and appropriate.

**Attention:**

- Do not reveal the ground truth in the Judgement!
- Always prioritize the locate tool when obtaining a bounding box.
- The judgement should be clear, brief, concise, and constructive.

### Complete Examples:

**\*\*Example 1\*\* (Correct example)**  
 Question: What does this sign signify?  
 Ground truth: do not enter  
 Predicted answer: do not enter  
 Visual search process: The visual search follows a structured process to determine the sign's meaning. It locates the sign using an object detection tool, which identifies the bounding box as [112, 71, 411, 639]. The region is extracted and analyzed using a vision-language model (VLM), which provides the answer "do not enter".  
 Judgement: The predicted answer is correct. The visual search process is reasonable.

**\*\*Example 2\*\* (Incorrect example)**  
 Question: What does this sign signify?  
 Ground truth: do not enter  
 Predicted answer: do not  
 Visual search process: The visual search follows a structured process to determine the sign's meaning. It locates the sign using an object detection tool, identifies the bounding box as [112, 71, 411, 639], extracts the region, and applies a VLM to analyze the content. The VLM's response is "do not".  
 Judgement: The predicted answer is incorrect. The steps in the visual search process are reasonable.

**\*\*Example 3\*\* (Incorrect example)**  
 Question: What does this sign signify?  
 Ground truth: do not enter  
 Predicted answer: Stop  
 Visual search process: The visual search follows a structured process to determine the sign's meaning. It locates the sign using an object detection tool, identifies the bounding box as [112, 71, 411, 639], extracts the region, and applies a VLM to analyze the content. The VLM's response is "Stop", suggesting the sign is a stop sign.  
 Judgement: The predicted answer is incorrect. The steps in the visual search summary are reasonable. The sign's bounding box [112, 71, 411, 639] already includes the correct answer according to the image content. However it does not answer correctly, maybe you does not understand the image content correctly.

**\*\*Example 4\*\* (Incorrect example)**  
 Question: What does this sign signify?  
 Ground truth: do not enter  
 Predicted answer: no smoking  
 Visual search process: The visual search follows a structured process to determine the sign's meaning. It locates the sign using an object detection tool, identifies the bounding box as [112, 71, 411, 639], extracts the region, and applies a VLM to analyze the content. The VLM's response is "no smoking".  
 Judgement: The predicted answer is incorrect. The steps in the visual search summary are reasonable. The answer region is not correctly located in [112, 71, 411, 639]. So you locate the wrong area.

### Provide the Judgement for the following:

Figure 9: The judgement prompt in our verification tool.

You are an AI expert. You are given the image, the question, the ground truth, the student's predicted answer, their visual search process, the judgment of that answer and process, and previous feedback.  
 If there are red bounding boxes in the image, they are the final answer regions in the visual search process.

Your task is to provide one **\*\*new and specific\*\*** piece of feedback to help the student improve their visual search process, identify the correct answer region, and answer the question more accurately.

Your feedback may fall into one of the following categories:

- 1) **\*\*New Search Strategy\*\***: Give a new search strategy to find the answer region. Identify what the answer region is near or which part of the image it is located in.
- 2) **\*\*Adjust the Bounding Box\*\***: If the red bounding box is close to the ground truth region, explain how to refine the bounding box (e.g., enlarge or narrow).
- 3) **\*\*Answer Correction Guidance\*\***: If the region is correct but the answer is wrong, help the student interpret the content based on visible evidence.

Requirements:

- Do not reveal the ground truth in the feedback.
- The feedback must be **\*\*new\*\*** and should not repeat previous feedbacks.
- Ensure the feedback is direct, helpful, and actionable in helping the student find the correct answer region.
- Keep your feedback clear, specific, and constructive. Avoid vague or general statements.
- Since the student's observation of the image content is limited, please provide feedback based on the image content visible to the student.
- Use the guide lines to infer the object's likely position and size, but express them only as relative proportions—do not give absolute numbers.

### Complete Examples:

**\*\*Example 1\*\***  
 Question: What does this sign signify?  
 Ground truth: do not enter  
 Predicted-answer: do not  
 Visual search process: The visual search follows a structured process to determine the sign's meaning. It locates the sign using an object detection tool, identifies the bounding box as [112, 71, 411, 639], extracts the region, and applies a VLM to analyze the content. The VLM's response is "do not".  
 Judgement: The predicted answer is incorrect. The steps in the visual search process are reasonable. But the red bounding box [112, 71, 411, 639] is not the correct answer region, it partially includes the correct answer region.  
 Feedback: The sign's bounding box [112, 71, 411, 639] already includes part of the correct answer according to the image content. Enlarge the bounding box [112, 71, 411, 639] to include the complete sign.

**\*\*Example 2\*\***  
 Question: What does this sign signify?  
 Ground truth: : do not enter  
 Predicted-answer: no smoking  
 Visual search process: The visual search follows a structured process to determine the sign's meaning. It locates the sign using an object detection tool, identifies the bounding box as [112, 71, 411, 639], extracts the region, and applies a VLM to analyze the content. The VLM's response is "Stop", suggesting the sign is a stop sign.  
 Judgement: The predicted answer is incorrect. The steps in the visual search summary are reasonable. The sign's bounding box [112, 71, 411, 639] already includes the correct answer according to the image content. However it does not answer correctly, maybe you does not understand the image content correctly.  
 Feedback: The sign's bounding box [112, 71, 411, 639] already includes the correct answer according to the image content. However, it does not answer correctly, so please narrow down the bounding box [112, 71, 411, 639] to focus on the sign's text part to further analyze the sign's meaning.

**\*\*Example 3\*\***  
 Question: What is the color of the shoes wearing by the woman in black?  
 Ground truth: black  
 Predicted-answer: red  
 Visual search process: The visual search follows a structured process to determine the woman's meaning. It locates the woman using a detection tool, identifies the bounding box as [112, 71, 411, 639], extracts the region, and applies a VLM to analyze the content. The VLM's response is "red".  
 Judgement: The predicted answer is incorrect. The steps in the visual search process are reasonable. The answer region is not correctly located in [112, 71, 411, 639]. So you locate the wrong area.  
 Feedback: You find the wrong person, the woman in black is not the person you want to find. The woman in black is standing to the left of the building, so you can find the building, and focus the area to the left of the building.

### Provide one simple and clear feedback(no need to be overly specific, and no need to much details) for the following:  
 (Ensure the feedback differs from previous evaluation feedbacks!!!)

Figure 10: The feedback prompt in our verification tool.

You are an AI assistant. Given an image region and a specific problem, Your task is to provide an accurate solution that can solve the problem.

Solution includes:

- Reasoning: Analyze the image content to determine the best approach to solve the problem.
- Suggestion: Provide clear step-by-step instructions to solve the problem based on the image content and reasoning.

Requirements:

1. Be simple, clear, and precise—avoid unnecessary details or vague terms.
2. Ensure each step should use and start with tools: "Locate" "Adjust\_bbox", or "VLM".
  - \* Locate tool: should locate a specific object, like "a red apple" or "a dog" in the image, not general object, like "small object" or "small area",
  - Avoid locating an object that is nearly the same size as the small region.
  - Always prioritize the locate tool when obtaining a bounding box.

Possible solutions include:

- Identify one clear, unambiguous landmark near the target object or area to solve the problem.
- Adjust the bounding box by enlarging or narrowing it.
- If the image lacks sufficient detail, use your knowledge or common sense to infer the object's likely location and approximate extent, such as which object it might be near or which region of the image it might appear in.

For example:

Problem: Can not identify the breed of the dog from the whole dog bounding box [100, 100, 200, 200]. Provide you the bounding box area [100, 100, 200, 200]. Please infer which part of the dog contains more distinctive features for breed identification.  
 Solution:  
 - Reasoning: Based on the image content in bounding box [100, 100, 200, 200] and the knowledge, the dog's head contains more distinctive features for breed identification, such as ear shape and nose/mouth area.  
 - Suggestion: First locate the dog's head area in the bounding box [100, 100, 200, 200]; Second, carefully observe its ears and nose/mouth to determine the breed.

Problem: Can't locate the sign in the red box [120, 120, 150, 150] (building). I've provided the full image; any suggestions on finding the sign?  
 Solution:  
 - Reasoning: Based on the image content, the sign is around the red box, so you can enlarge the bounding box of the red box to get the area around the red box to locate the sign.  
 - Suggestion: First, enlarge the bounding box [120, 120, 150, 150]. Second, locate the sign in the enlarged bounding box.

Problem: Can not locate the plane in the whole image. Provide you the whole image, Please infer which part of the image may contain the plane.  
 Solution:  
 - Reasoning: Based on the image content, an airplane is found around the runway or an open area with linear markings.  
 - Suggestion: First locate the grassy area with white parallel lines; Second, enlarge the bounding box of the grassy area to get the area around the grassy area to locate the airplane; Third, locate the airplane around the grassy area.

Problem: Can not locate the cup in the whole image. Provide you the whole image, Please infer which part of the image may contain the cup.  
 Solution:  
 - Reasoning: Based on the image content, can not find the cup, but it is commonly put on the red table.  
 - Suggestion: First locate the red table; Second, locate the cup in the red table's bounding box.

Please directly provide one brief and clear solution based on the following information:

Figure 11: The prompt used for VLM reasoning in our understanding tool.

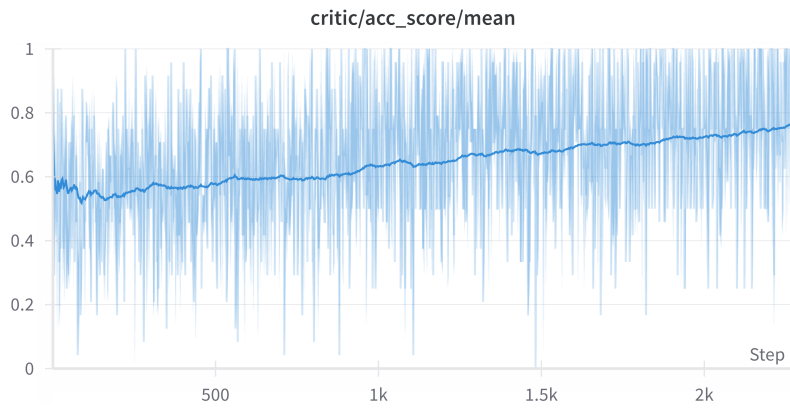


Figure 12: Mean Accuracy Over RL Training Steps.

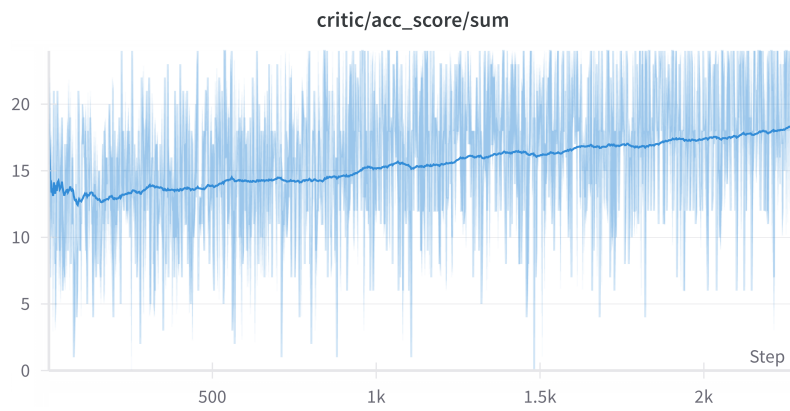


Figure 13: Accuracy Sum Over RL Training Steps.

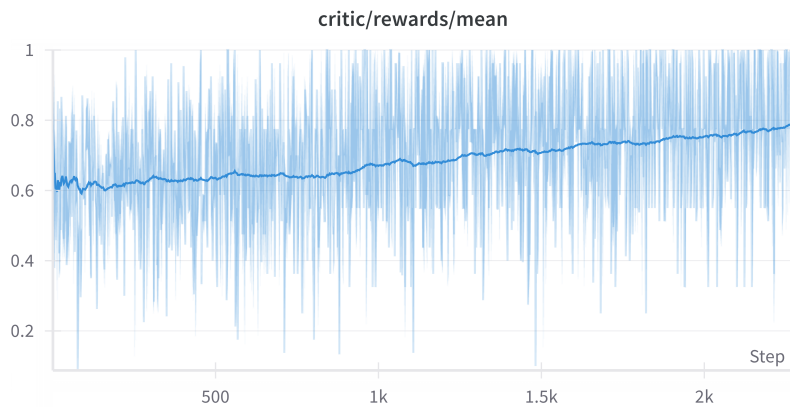


Figure 14: Rewards Over RL Training Steps.

## C Benchmark details

We evaluate our model on various MLLM benchmarks. Here is a detailed analysis of these benchmarks:

**V\* Bench** is a benchmark specifically designed to assess the ability of MLLMs to process high-resolution images and focus on fine visual details. The dataset consists of 191 samples. It targets scenarios where models must answer questions about extremely small objects in the image. Unlike standard benchmarks, V\* emphasizes the importance of dynamic visual search capabilities, requiring multimodal models to accurately identify and ground subtle visual information that static vision encoders might easily overlook.

**TextVQA** evaluates the model’s capability to extract and understand textual information embedded within images. This dataset contains 5,000 samples. This benchmark includes scenarios such as reading text from road signs, documents, or digital screens. We adopt the standard evaluation split and focus on questions where the answers rely on text present in the visual input. Metrics such as exact match accuracy and token-level overlap are used to gauge performance.

**m3cot** is a newly proposed benchmark aimed at advancing research in multi-modal, multi-step, and multi-domain chain-of-thought (CoT) reasoning. Unlike previous MCoT benchmarks that are limited by shallow reasoning depth and domain coverage, M<sup>3</sup>CoT introduces diverse tasks requiring step-by-step reasoning across both textual and visual modalities, covering domains such as science, daily life, and medicine. To enable fine-grained evaluation, M<sup>3</sup>CoT provides richly annotated reasoning trajectories. Experiments show that while current vision-language models (VLLMs) perform well on simpler datasets, they struggle on M<sup>3</sup>CoT, highlighting a significant gap between model and human-level reasoning.

**POPE** is a benchmark dataset specifically designed to evaluate whether large vision-language models (LVLMs) generate object hallucinations, where the model describes objects that are not actually present in the image. The benchmark contains 9,000 carefully curated samples, each consisting of an image and a set of object-centric questions. Some questions refer to objects that are truly present in the image, while others are intentionally crafted to reference objects that do not exist, in order to test the model’s grounding ability.